Tunable deep ultraviolet single-longitudinal-mode laser generated with $Ba_{1-x}B_{2-y-z}O_4Si_xAl_yGa_z$ crystal

Rui Wang,[1] Hao Teng,[1,3] Nan Wang,[1] Hainian Han,[1] Zhaohua Wang,[1] Zhiyi Wei,[1,4] Maochun Hong,[2] and Wenxiong Lin[2]

[1]*Beijing National Laboratory for Condensed Matter Physics, Institute of Physics, Chinese Academy of Sciences, Beijing 100190, China*

[2]*Fujian Institute of Research on the Structure of Matter, Chinese Academy of Sciences, Fuzhou 350002, China*

[3]*e-mail: hteng@iphy.ac.cn*

[4]*e-mail: zywei@iphy.ac.cn*

Received January 7, 2014; revised March 1, 2014; accepted March 4, 2014; posted March 4, 2014 (Doc. ID 204325); published March 28, 2014

We report a new nonlinear crystal, $Ba_{1-x}B_{2-y-z}O_4Si_xAl_yGa_z$, and employ it to a compact 1 kHz single-longitudinal-mode Ti:Sapphire master oscillator power amplifier system for fourth harmonic generation. A maximum output power of 130 mW is obtained in the tunable range of 195–205 nm with linewidth of less than 0.1 pm. © 2014 Optical Society of America

OCIS codes: (140.3570) Lasers, single-mode; (140.3610) Lasers, ultraviolet; (190.4380) Nonlinear optics, four-wave mixing; (140.3600) Lasers, tunable; (190.2620) Harmonic generation and mixing; (140.3280) Laser amplifiers.

http://dx.doi.org/10.1364/OL.39.002105

The generation of tunable deep-ultraviolet (DUV) coherent light with narrow linewidth using a nonlinear crystal is an intensive research topic, due to the widespread potential applications in many fields [1–6]. In past decades, dye lasers have even been used as a primary DUV source with tunable narrow-bandwidth pulse output [7], but the possible applications are limited because of the poor beam quality, low pulse energy, short lifetimes of dye solutions, amplified spontaneous emission, and toxic chemicals. Thanks to the continuous efforts made over the last twenty years, remarkable progress has been made on narrow linewidth DUV coherent radiations by nonlinear frequency conversion of diode-pumped solid state lasers (DPSSLs) with nonlinear crystals, such as β-BaB_2O_4 (β-BBO), LiB_3O_5 (LBO), BiB_3O_6 (BiBO), $CsLiB_6O_{10}$ (CLBO), and $KBe_2BO_3F_2$ (KBBF), etc. For example, a tunable 8 mW DUV radiation with spectrum bandwidth of 0.1 nm over the entire range of 198–300 nm at repetition rate of 10 Hz using β-BBO was reported by Meguro *et al.* in 1994, [1]. By 2000, Sakuma *et al.* had reported a 5 kHz DUV laser system by efficient use of CLBO crystal, which produced 1.5 W at 196.3 nm light with linewidth less than 200 MHz [2]. In 2001, Togashi *et al.* further obtained vacuum ultraviolet (VUV) radiation at 153 nm in a Xe gas cell by a tunable 5 kHz Ti:Sapphire laser system, with a typical linewidth of 1.9 GHz and pulse duration of 0.6 ns [3]. One year later, the same group obtained 0.6 mW, single-longitudinal-mode (SLM), 157 nm coherent radiation at 1 kHz with linewidth of <0.008 pm, based on a Ti:Sapphire master oscillator power amplifier (MOPA) system [4]. Since the nonlinear crystal KBBF was invented, DUV coherent light has been obtained directly through second harmonic generation (SHG). Several narrow linewidth DUV laser systems have already adopted this in their final nonlinear process [5,6]. In 2008, H. Zhang *et al.* reported a 175–210 nm widely tunable narrow linewidth DUV light generated from KBBF [5]. The maximum output power was 2.23 mW at 193 nm with the linewidth of less than 2 nm. Later, Ito *et al.* demonstrated a 0.2 W, line-narrowing DUV (193 nm) coherent radiation, operating at the repetition rate of 6 kHz, with a prism-coupled KBBF device [6]. However, the thickness-limited growth of KBBF effectively prevents SHG from nanosecond pulses, especially in the case of high incident power.

In this Letter, a new nonlinear crystal $Ba_{1-x}B_{2-y-z}O_4Si_xAl_yGa_z$ ($x = 0$–0.15, $y = 0$–0.01, $z = 0$–0.04, $x^2+y^2+z^2 \neq 0$, BBSAG) is introduced as an optimized β-BBO, and employed in the final sum frequency mixing (SFM) stage of a compact tunable SLM–DUV laser system, which consists of an auto-synchronized 1 kHz Ti:Sapphire MOPA system [8] and a three-step frequency conversion chain. The DUV radiation with the spectrum linewidth of <0.1 pm and pulse duration of 7.8 ns (FWHM) in the wavelength-tunable range of 195–205 nm is generated and the maximum output power of 130 mW is obtained at 201 nm.

BBSAG crystal represents a trigonal system, with $C_3^4 - R_3$, which is a kind of low-temperature phase barium metaborate single crystal, doped with one or more elements selected from Si, Al, and Ga. Chen invented this new nonlinear crystal to overcome the shortcoming of deliquescence of β-BBO and enhance the frequency doubling effect, hardness, and optical threshold; in addition, he has measured the properties of different doping formula BBSAG samples and compared them with β-BBO [9]. As shown in Table 1, all BBSAG samples were almost completely non-deliquescent during about one month of constant humidity, and its hardness, optical threshold, and SHG efficiency were improved greatly compared with β-BBO. In addition, a preferably molten salt method, or flux Czochraksi method is also invented for large-size BBSAG single-crystal growth. As introduced in Ref. [9], a single-crystal BBSAG can grow to beyond 10 mm in thickness.

To further understand the nonlinear characteristics of BBSAG in the DUV region, we comparatively measured the transmittance spectrum, refractive indices, and phase matching angles of the SHG for BBSAG (10 mm thickness) and β-BBO, with the same length. As shown in Fig. 1, the BBSAG crystal has almost the same

Table 1. Deliquescence, Hardness, Damage Threshold, and SHG Efficiency Comparisons Between BBSAG and β-BBO

	Change Rate of Max Output Power of SHG after 34 days Constant Humidity Experiment[a]	Mohs Hardness	Optical Threshold[a]	SHG Efficiency
BBSAG[b]	0	6	23.65 J/cm^2, 3365.2 MW/cm^2	25% higher than β-BBO
β-BBO	Fell by 71%	4	12.67 J/cm^2, 1809.7 MW/cm^2	—

[a]Laser source: 1064 nm Q-switch YAG laser with pulse duration of 7 ns and energy of 895 mJ; crystal thickness: ~3 mm.
[b]Different samples of BBSAG present similar results.

transmittance spectrum and short-wavelength absorption edge (~193 nm) as the β-BBO crystal. The refractive indices of ordinary light and extraordinary light for BBSAG at several different wavelengths were measured and fitted. In Fig. 2 we can see that the refractivity curves of BBSAG are almost the same as those of β-BBO. Then, the Sellmeier equations of the BBSAG crystal are derived according to the measured refractive indices (Eq. 1)

$$\begin{cases} n_o^2 = 2.7134 + \frac{0.024925}{\lambda^2 - 0.0044118} \\ n_e^2 = 2.3649 + \frac{0.014811}{\lambda^2 - 0.0095538} \end{cases}. \quad (1)$$

Here the unit of λ is micrometer. Figure 3 presents the change of calculated SHG phase matching angle of BBSAG with wavelength, and the inserted figure shows the change in the DUV region. It is found that the SHG phase matching angles of BBSAG and β-BBO are almost the same. Based on the optical performances measured and calculated above, BBSAG can be used in any frequency conversion system as β-BBO; thus, we cut the BBSAG crystal at the same phase matching angle as β-BBO in our experiment.

Figure 4 is the sketch of our tunable SLM–DUV system, including a SLM Ti:Sapphire oscillator followed by a four-pass amplifier and three-step nonlinear frequency conversion unit for fourth harmonic generation (FHG). A typical self-seed-injected Littman-type configuration is adopted for the Ti:Sapphire oscillator [4,10,11], which consists of a flat dichromatic end mirror, a grating, a flat total reflector facing the direction of −1 st-order diffraction, and a flat output coupler. The dichromatic end mirror is high reflective- (HR-) coated at 765–835 nm and anti-reflective- (AR-) coated at 520–540 nm, and is used for coupling the pump laser into the cavity. The grating (Optomatrix Inc.), with a groove density of 1800 lines/mm, is placed at a grazing incident angle of 1.5°. The total reflector, with the same size grating, can be horizontally tuned by a mirror mount with piezo motor actuators (Picomotor 8302) to change the oscillating wavelength. The resolution of tunable wavelength of the output laser is less than 50 MHz. The flat output coupler is coated in the range of 765–835 nm, with reflectivity of 70%. A 4-mm-thick Ti:Sapphire crystal, with absorption factor of 6.66, is placed 10 mm away from the end mirror in the cavity, which was cooled at 15°C by water. The oscillator has two cavities: a dispersive cavity and a gain cavity. The dispersive cavity consists of the end mirror and the grating and reflector for providing SLM seed. The gain cavity consists of the end mirror, the grating, and the output coupler for providing gain of the SLM pulse. The cavity lengths of the dispersive cavity and the gain cavity are 65 and 160 mm, respectively.

A zigzag-type confocal configuration is employed for the four-pass amplifier, which consists of two flat folding 0° reflecting mirrors (M_1, M_2), two concave 0° reflecting mirrors with curvature radii of 2000 mm (M_3, M_4), and four 45° reflectors (M_5, M_8). A 10-mm-thick Ti:Sapphire crystal with absorption factor of 5.04 is placed at the focus point of M_1/M_2, which is cooled by liquid nitrogen.

The SLM oscillator and the four-pass amplifier are together pumped by a 26.5 W, 1 kHz frequency-doubled Nd:YLF laser (DM 30-527, Photonics Industries Inc.), which is divided by beam splitter (BS) with reflectivity of 80%, after beam expansion. The transmission part of the pump laser is coupled into the oscillator through the end mirror by a lens (F_1) with a focal length of 200 mm and the reflection part of the pump laser is focused into the amplifier by a lens (F_2) with a focal length of 500 mm. The spot sizes of the pump beam on the crystals in the oscillator and the amplifier are 240 μm and 600 μm, respectively, which are matched with the size of the beam waist in the cavities. As discussed in Ref. [8], since the pulse build-up time of the oscillator is about 80 ns, auto-synchronization of the seed pulses and the pump pulses in the amplifier's Ti:Sapphire crystal can be achieved.

The seed pulses from the oscillator have a linewidth of 0.4 pm, with tunable wavelength range of 780–820 nm and energy of 550 μJ. The typical interference fringe of the spectral linewidth measured by a commercial wavelength meter (WS-7, Highfinesse GmbH) is shown

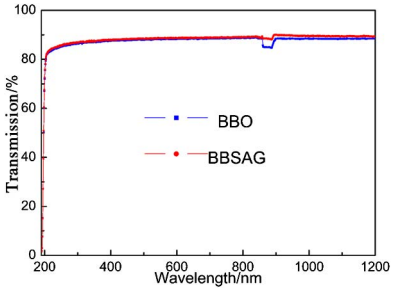

Fig. 1. Transmittance spectra of BBSAG and β-BBO.

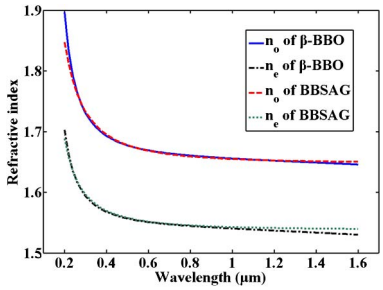

Fig. 2. Refractive indices of BBSAG and β-BBO.

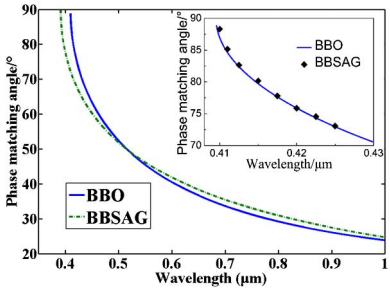

Fig. 3. Phase matching angles of BBSAG and β-BBO at the wavelength of SHG for Type I.

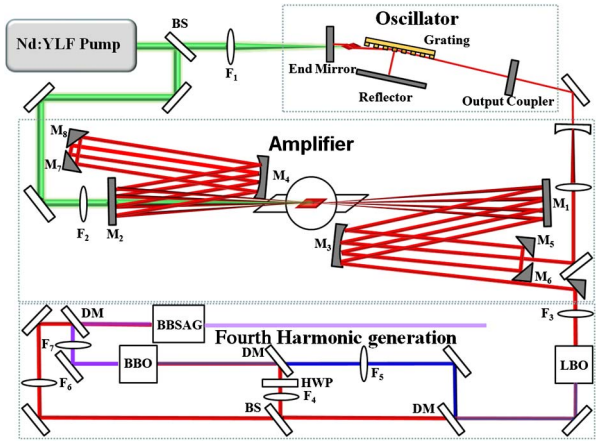

Fig. 4. Schematic experimental setup of auto-synchronized SLM Ti:Sapphire MOPA system and FHG unit (HWP, half-wave plate; BS, beam splitter; DM, dielectric mirror).

in Fig. 5. The linewidth is kept almost the same across the tunable range of 780–820 nm, as well as from the amplifier. The power of the seed is further amplified to a maximum 6.5 W under the remaining pumping power of 21.2 W transmitting through the BS while the pulse duration is stretched to 19.2 ns after four-pass amplification. From Fig. 6, we can see that the pulse is not only stretched, but also deformed from Gaussian shape to a flattened-Gaussian-like shape. This is because the optical path between adjacent passes in the amplifier is not long enough to separate the falling edge of the former pass and the rising edge of the latter pass; thus, the pulse is self-overlapping. The beam quality of the output pulse from the amplifier was measured by a commercial M^2 analyzer (M^2-200s, Spiricon Inc.). As shown in Fig. 7, M_x^2 is equal to 1.442 and M_y^2 is equal to 1.300. The far-field beam profile is shown in the inserted figure.

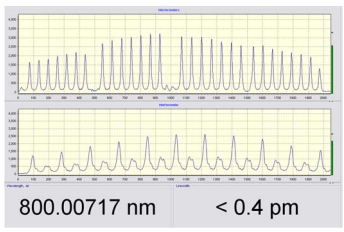

Fig. 5. Measured linewidth of amplified pulse at wavelength of 800 nm.

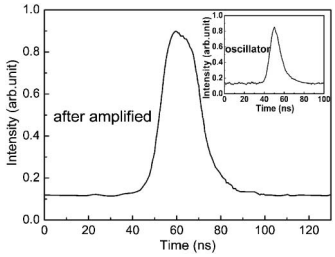

Fig. 6. Pulse durations of the output pulses from the oscillator (inserted) and the amplifier.

As shown in Fig. 4, a three-step nonlinear frequency conversion chain, including a SHG process and two SFM processes, is used to generate a 195–205 nm tunable pulse. First, the amplified fundamental wave (FW) is focused by a 600 mm focus-length lens (F_3) in a 14 mm thickness type I LiB_3O_5 crystal (cut at $\theta = 90°$, $\varphi = 31.7°$). The generated second harmonic and the remaining FW are split by a dichroic mirror. The transmitting FW is divided into two parts by a BS with 80% reflectivity at 780–820 nm for third harmonic generation (THG) and FHG. The reflecting part of the FW is 90° polarization rotated to parallel to SHG by a broad-band HWP and further focused onto a 14 mm thickness type I β-BBO crystal (cut at $\theta = 44.3°$, $\varphi = 0°$) by 600 mm focus-length lens (F_4), combined with the SHG, which is focused by a 400 mm focus-length lens (F_5) to generate THG. The THG and the transmitting part of the FW are focused into a 9.948 mm thickness type I BBSAG crystal (cut at $\theta = 64.8°$, $\varphi = 0°$) by a 300 mm focus-length lens (F_7) and a 400 mm focus-length lens (F_6) to generate FHG. During the two SFM processes, for increasing the beam overlapping ratio in the crystals, collimating lenses and beam shaping lenses are inserted before the focus lenses to compensate the beam profile distortion caused by the spatial walk-off in the previous nonlinear processes.

The real linewidth of FHG is estimated to be less than 0.1 pm from FW, since the wavelength of FHG is beyond the measuring range of the wavelength meter. The wavelength tunable output of FW, SHG, THG, and FHG can be obtained by horizontal tilting the reflector in the oscillator and the angle of nonlinear crystals. As shown in Fig. 8, the output power of FW, SHG, and THG are almost kept the same in the main tunable wavelength ranges (780–820 nm, 390–410 nm, and 260–274 nm). However, the output power of FHG drops sharply when the wavelength out of the 198–203 nm range, due to the serious phase mismatch and walk-off in the FHG–BBSAG during the

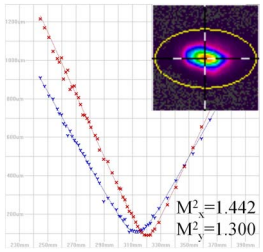

Fig. 7. Beam quality of the fundamental light from the amplifier.

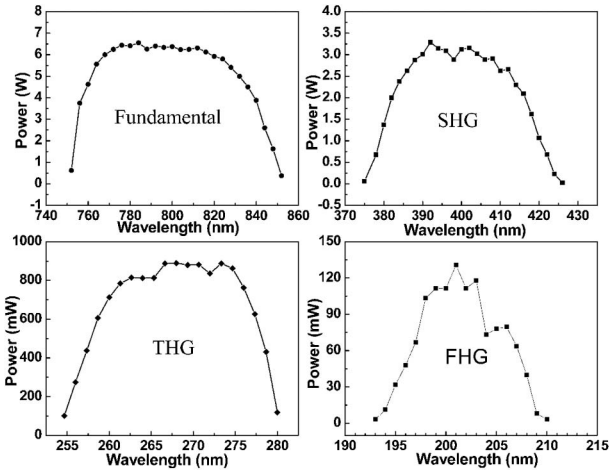

Fig. 8. Tunable output powers of FW, SHG, THG, and FHG under maximum pumping power.

tuning process. Figure 9 shows the output power and conversion efficiency for each stage at the wavelength where the maximum FHG efficiency can be reached. The maximum output power of SHG, THG, and FHG are 3.1 W, 890 mW, and 130 mW, respectively, corresponding to optical-to-optical conversion efficiencies of 50.5%, 28.3%, and 14.6% from the previous stage. Under the same experimental conditions, a 10-mm-thickness type I β-BBO (cut at $\theta = 64.8°$, $\varphi = 0°$) is used instead of BBSAG at the last stage, for comparison. The maximum output power of FHG generated in the β-BBO crystal is 110 mW, which is lower than that from BBSAG. The experimental results illustrate that BBSAG can provide higher SFM efficiency than β-BBO in the DUV region. It is important to notice that, to obtain the optimum SFM efficiency, a low numerical aperture focusing system was adopted in our experiment, to attenuate walk-off during the FHG process; thereby, the intensity of FW on BBSAG is only ~200 MW/cm^2. Considering the high damage threshold of BBSAG, higher output power and conversion efficiency can be expected if a higher energy input pulse is used.

In conclusion, we have developed a compact tunable SLM–DUV source, based on a BBSAG crystal with spectral linewidth of <0.1 pm. The maximum power of 130 mW at 201 nm is obtained in a tunable range of 195–205 nm. The experimental results show that, as a new nonlinear crystal with non-deliquescence and a high damage threshold, BBSAG has higher SFM efficiency than β-BBO in the DUV region. Moreover, it has almost the same optical characteristics as β-BBO, i.e., transmittance spectrum, refractive indices, and phase matching angle; thus, this crystal demonstrates great

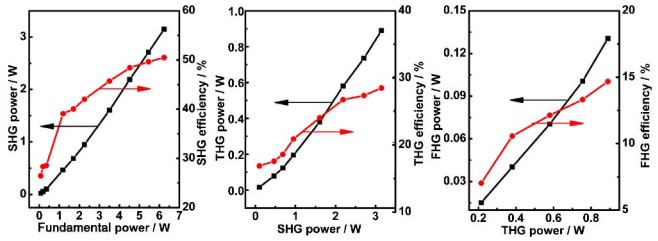

Fig. 9. Output power and conversion efficiency of SHG, THG, and FHG as a function of the input power of FW, SHG, and THG. All data are measured at the fundamental wavelength of 804 nm.

potential for nonlinear optics applications, especially in the DUV region. In addition, considering its centimeter growth size, BBSAG can also be regarded as an important supplement of KBBF for nanosecond DUV pulse generation.

We thank the helpful discussion with Prof. Bingbing Wang and Li Dehua. This work was partly supported by the National Key Basic Research Program of China under Grant No. 2013CB922401 and the National Natural Science Foundation of China under Grants Nos. 91126008 and 11074298.

References

1. T. Meguro, T. Caughey, L. Wolf, and Y. Aoyagi, Opt. Lett. **19**, 102 (1994).
2. J. Sakuma, K. Deki, A. Finch, Y. Ohsako, and T. Yokota, Appl. Opt. **39**, 5505 (2000).
3. T. Togashi, N. Nabekawa, T. Sekikawa, and S. Watanabe, Opt. Lett. **26**, 831 (2001).
4. T. Suganuma, H. Kubo, O. Wakabayashi, H. Mizoguchi, K. Nakao, Y. Nabekawa, T. Togashi, and S. Watanabe, Opt. Lett. **27**, 46 (2002).
5. H. Zhang, G. Wang, L. Guo, A. Geng, Y. Bo, D. Cui, Z. Xu, R. Li, Y. Zhu, X. Wang, and C. Chen, Appl. Phys. B **93**, 323 (2008).
6. S. Ito, T. Onose, K. Kakizaki, T. Matsunaga, J. Fjimoto, H. Mizoguchi, S. Watanabe, C. Zhou, T. Kanai, Y. Kobayashi, C. Chen, and X. Wang, *Lasers, Sources, and Related Photonic Devices Technical Digest* (Optical Society of America, 2012), paper AT4A.7.
7. W. Ulbachs, K. S. E. Eikema, and W. Hogervorst, J. Opt. Soc. Am. B **14**, 2469 (1997).
8. R. Wang, N. Wang, H. Teng, and Z. Wei, Appl. Opt. **51**, 5527 (2012).
9. C. Z. Chen, "Doped low temperature phase BaB_2O_4 single crystal the manufacturing method thereof and wave changing elements therefrom," European patent application, EP 2 322 697 A (2010).
10. D. Ko, G. Lim, S. Kim, B. H. Cha, and J. Lee, Opt. Lett. **20**, 710 (1995).
11. A. J. Merrian and G. Y. Yin, Opt. Lett. **23**, 1034 (1998).